ZIBELINE INTERNATIONAL™ PUBLISHING

ISSN: 2521-2915 (Print)
ISSN: 2521-2923 (Online)
CODEN: PJGABN

Pakistan Journal of Geology (PJG)

DOI: http://doi.org/10.26480/pjg.01.2026.12.21

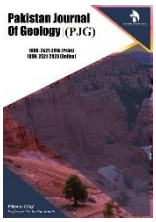

RESEARCH ARTICLE

UTILIZING REMOTE SENSING AND GIS TO EVALUATE GROUNDWATER POTENTIAL IN GOMBE AND THE SURROUNDING AREA, NORTHEASTERN NIGERIA

Ogechukwu H. Obimba[a,b*], Adeleye Y. B. Anifowose[c], and Kola A. N. Adiat[c]

[a] COPINE, Obafemi Awolowo University, Ile-Ife, Osun State, Nigeria.
[b] Department of Remote Sensing and Geoscience Information System, Federal University of Technology, Akure, Nigeria
[c] Department of Applied Geophysics, Federal University of Technology, Akure, Ondo State, Nigeria
**Corresponding Author Email: ogeobimba@yahoo.com*

ARTICLE DETAILS

Article History:

Received 26 January 2026
Revised 20 February 2026
Accepted 25 February 2026
Available online 10 March 2026

ABSTRACT

Increasing population growth, domestic and agricultural water demand have heightened reliance on groundwater in Gombe and its environs. Proper management of this resource needs both systematic and spatial evaluation. This study integrates Remote Sensing (RS), Geographic Information System (GIS), and the Analytic Hierarchy Process (AHP) to delineate groundwater potential zones in a geologically heterogeneous area. Eight groundwater-influencing parameters: geology, lineament density, slope, drainage density, soil, land use/land cover, elevation, and rainfall were weighted through AHP and analysed in ArcGIS 10.8 to generate groundwater potential map. The resulting map shows a classification of high, moderate, low, and very low potential zones. High-potential zones align with the Gombe, Bima and Sandstone formations, characterized by gentle slopes, lower drainage density, and enhanced fracture development, whereas low-potential zones are predominantly associated with crystalline basement terrains, which exhibit steep gradients and impervious kerri kerri formation. Model validation using borehole yield data produced an Area under the Curve (AUC) value of 0.84, indicating strong predictive accuracy. The study shows that the integration of RS parameters in GIS and AHP provides a reliable and cost-effective framework for groundwater potential assessment, supporting sustainable groundwater development and management in semi-arid, data-constrained regions. Beyond conventional RS–GIS analysis, this study integrates artificial intelligence techniques specifically the Analytic Hierarchy Process (AHP) for factor weighting and ROC–AUC machine learning validation to enhance predictive accuracy and reduce subjectivity in groundwater potential mapping.

KEYWORDS

Semi-Arid Region; RS/GIS; Upper Benue Trough; ROC-AUC machine learning metrics

1. INTRODUCTION

In arid and semi-arid regions, limited rainfall and high evapotranspiration makes groundwater the primary source of freshwater for domestic and agricultural use (Todd and Mays, 2004). Rapid population growth and increasing climate change has put pressure on groundwater resources, necessitating the need for efficient exploration and management (Abdullahi and Saidu, 2020). Conventional field-based groundwater investigation methods are usually costly, spatially challenged, and unable to capture subsurface variability at wide scale especially in a heterogeneous terrain.

Remote Sensing (RS) and Geographic Information Systems (GIS) provides a cheaper means of evaluating hydrogeological conditions over large areas by integrating geomorphology, terrain, and land surface characteristics (Shalaby and Tateishi, 2007; Mulder et al., 2011). When aided by the Analytic Hierarchy Process (AHP), these tools allow systematic consideration of controlling factors influencing groundwater occurrence (Saaty, 1980; Kumar and Krishna, 2018).

In Gombe and environs, assessing groundwater is a problem due to complex geological transitions between basement and sedimentary units, limited subsurface data, which leads to frequent borehole failure. Previous RS–GIS-based studies in the area were conducted at basin scales and often used limited thematic layers without detailed validation. This reduces their applicability and wide usage for serious groundwater planning.

This study employs an integration of Remote Sensing (RS), Geographic Information Systems (GIS), and Analytical Hierarchy Process (AHP) framework to delineate groundwater potential zones in Gombe and its environs. Eight hydrogeological parameters were considered and were subsequently validated using borehole yield data and Receiver Operating Characteristic (ROC) analysis. This approach provides improved insight into aquifer characteristics in a geologically complex, data-scarce setting, where groundwater occurrence exhibits spatial variability and erratic behaviour.

2. STUDY AREA

The study covers Gombe and neighbouring Akko, Kwami, and Yamaltu/Deba LGAs in northeastern Nigeria. It falls between latitude 10°14′52″–10°18′55″North, to longitude 11°06′24″–11°14′41″East, with an average area of 140 km^2. The terrain consists of undulating plains and isolated hills, drained mainly by the Gongola River, with the Dadin-Kowa Dam serving as a major source of water. It has a tropical wet-and-dry climate, receiving 850–1,000 mm of annual rainfall with temperatures of 25–32°C, and peak rainfall recharge occurring around August.

Quick Response Code	Access this article online	
	Website: www.pakjgeology.com	DOI: 10.26480/pjg.01.2026.12.21

Cite The Article: Ogechukwu H. Obimba, Adeleye Y. B. Anifowose, and Kola A. N. Adiat (2026). Utilizing Remote Sensing and Gis to Evaluate Groundwater Potential in Gombe and The Surrounding Area, Northeastern Nigeria. *Pakistan Journal of Geology, 10(1): 12-21.*

Geologically, the Precambrian Basement Complex rocks are overlain by Cretaceous sediments that host aquifers in weathered/fractured basement zones and in the Bima, Gombe, and sometimes the Kerri-Kerri sedimentary Formations. The Bima Sandstone provides the most productive aquifers, while shale and lateritic sedimentary layers locally limit groundwater storage. Fast population growth and raising water demand coupled with variable borehole yields over very short distances; highlight the need for improved groundwater potential assessment in the area. Figure 1.1 shows the stratigraphic succession of the upper Benue Trough, while Figure 1.2 is the study area map.

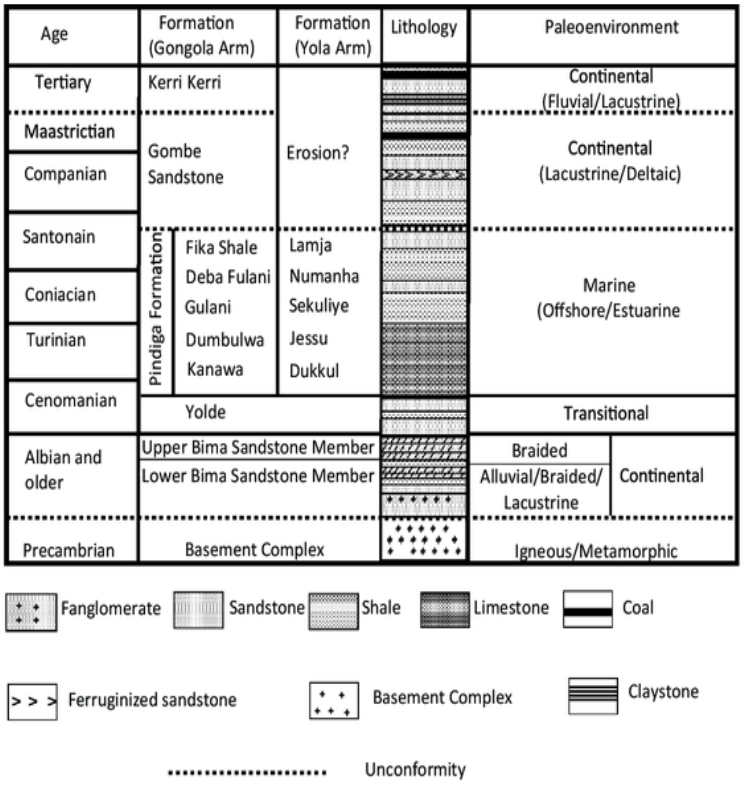

Figure 1: The stratigraphy of the upper Benue Trough (Abubakar et al., 2006)

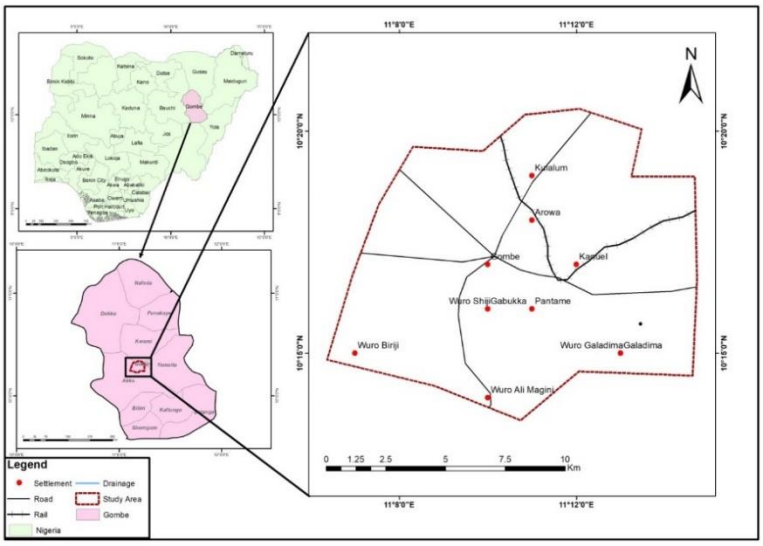

Figure 2: Location map of the study area.

3. Materials and Methods

3.1 Overview of Methodological Framework

The methodology adapted in the study involves integrating remote sensing and GIS workflow to delineate groundwater potential zones through multi-criteria spatial analysis. Eight thematic layers: lithology, lineaments, slope, drainage density, land use/land cover (LULC), soil, elevation and rainfall were derived from multispectral satellite imagery and DEM sources. Each parameter was reclassified according to its hydrogeological relevance in groundwater accumulation, and a relative weight assigned using the Analytical Hierarchy Process (AHP). The weighted layers were subsequently combined in a GIS through the weighted overlay analysis to produce the groundwater potential map.

The result was validated using borehole yield data and Receiver Operating Characteristic (ROC) analysis, from which the Area under the Curve (AUC) was computed to quantify predictive accuracy. The ROC curve plots the true positive rate (sensitivity) against the false positive rate (1 – specificity) across varying classification thresholds, providing a threshold-independent measure of model performance. The model achieved an AUC value of 0.84, indicating strong predictive accuracy and effective discrimination between productive and non-productive boreholes. This is consistent with reported benchmarks for GIS–AHP groundwater potential studies (Rahmati et al., 2016

Framework for this work is divided into five major stages: (i) data acquisition and preprocessing, (ii) derivation of thematic layers, (iii) AHP-based reclassification and weighting, (iv) weighted overlay analysis for groundwater potential mapping, and (v) model validation using borehole yield and ROC-AUC metrics (Figure 2.0).

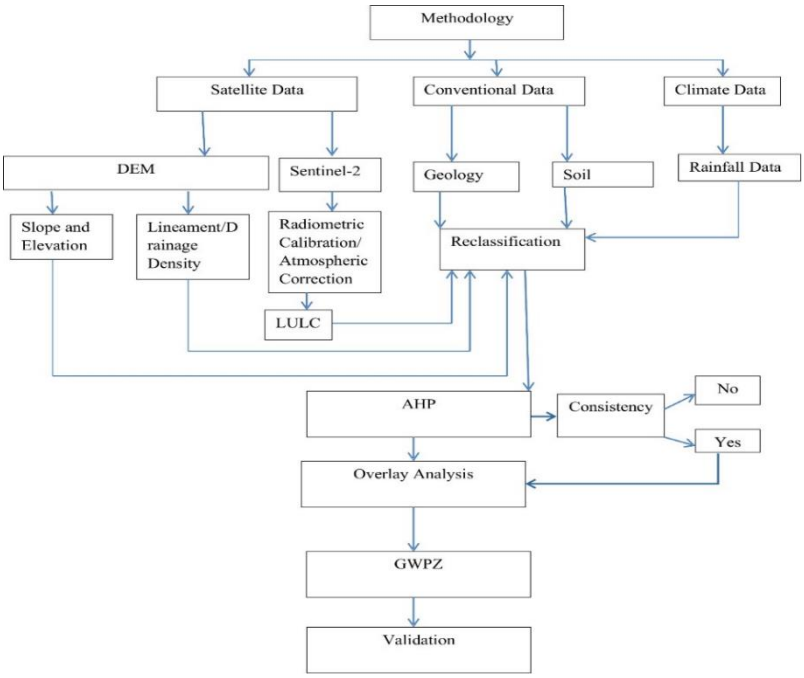

Figure 3: Methodological flow.

3.2 Data Acquisition and Preprocessing

Primary datasets included the Shuttle Radar Topography Mission (SRTM), Digital Elevation Model (DEM) and Sentinel-2A multispectral imagery. The DEM (30 m resolution) was sourced from the USGS Earth-Explorer platform, while Sentinel-2 data was acquired in August 2023 (minimal cloud cover). All datasets were projected to UTM Zone 32N (WGS 84 datum) to ensure spatial uniformity.

Atmospheric correction of the Sentinel-2A imagery was carried out using the Sen2Cor algorithm, and then Maximum Likelihood Supervised Classification (MLC) to generate a Land Use/Land Cover (LULC) map with five major classes: cropland, built-up area, scrubland, rock outcrop, and water bodies (Drusch et al., 2012). Terrain derivatives such as slope and drainage density were computed from the DEM using ArcGIS 10.8 spatial analysis tools.

Lineaments were extracted from DEM, then manually refined to minimise false positives. Lineament density was calculated using kernel density estimation (Nag and Lahiri, 2012). The IDW approach was used to interpolate continuous spatial variables, under the assumption that closeness between points reflects greater similarity (Burrough and McDonnell, 1998).

3.3 Analytical Hierarchy Process (AHP) Weighting

The relative importance of the eight conditioning factors was determined using AHP (Saaty, 1980). A pairwise comparison matrix was designed using expert judgment and literature review. Each factor was assigned a numerical value from 1 (equal importance) to 9 (extreme importance). The normalised eigenvector of the comparison matrix provided the final weights.

The Consistency Index (CI) and Consistency Ratio (CR) were computed using:

$$CI = \frac{\lambda max^{-n}}{n-1}, \text{CR} = \frac{CI}{RI}$$

Where λmax is the principal eigenvalue, *n* is the number of criteria, and RI is the Random Consistency Index. A CR < 0.1 indicates acceptable consistency. The computed CR of 0.011 confirmed the reliability of the weight matrix.

The Groundwater Potential Index (GPI) was then computed using a weighted linear combination:

$$GPI = \sum_{i=1}^{n} w_i * R_i$$

Where *wi* is the AHP-derived weight, and *Ri* is the reclassified rating of each factor.

3.4 Weighted Overlay and Groundwater Potential Zonation

In the Analytical Hierarchy Process (AHP), parameters are ranked and weighted based on their relative importance, priority, or influence on groundwater in the area. Ranking is done through pairwise comparisons (Table 1.0), while the weight represents the importance of each factor and is calculated from the pairwise comparisons and is usually expressed as a percentage or a decimal value. Lastly, the weights are normalised to sum to 100% (Table 1.0). All weighted thematic layers were overlaid in ArcGIS 10.8 using the Weighted Sum function to generate a composite Groundwater Potential Index (GPI) raster. The GPI was normalised to a 0–1 scale and classified into four potential zones: very low, low, moderate, and high based on natural breaks. The spatial distribution of these classes delineates areas with contrasting recharge potential and aquifer productivity.

Table 1: Ranking of factors

Criteria	Class	Rank	AHP Weight
A	Sandstone, Shale and Clay	3	0.071636
	Black shale, Siltstone sandstone, and Gypsum	4	
	Shale, Sandy clay and Calcerous sandstone	4	
	Coarse-grained granite, including Gneiss and Migmatite	3	
	Sandstone and Migmatite	1	

Table 1 (cont): Ranking of factors			
B	0.030 – 0.750 0.750 – 1.060 1.060 – 1.380 1.380 - 2.330	1 2 3 4	0.057930
C	0 – 20 20 – 50 50 – 70 70 - 100	4 3 2 1	0.123651
D	Built up Rock outcrop Cropland Shrubs land	4 3 2 1	0.024649
E	826.4 – 851.67 851.67 – 872.16 872.16 – 892.66 892.66 – 913.16	4 3 2 1	0.101736
F	0 – 0.86 0.86 – 2.79 2.79 – 5.08 5.08 – 8.15	4 3 2 1	0.022776
G	Leptosol unit Luvisol-cambisol unit Luvisol-leptisol unit	3 4 2	0.026722
H	Hills Valley Plains Pediment	4 1 2 3	0.021229

Where A is Geology, B is Drainage Density, C is Lineament Density, D is Land use and Land cover, E is Rainfall, F is Slope, G is Soil type, and H is Elevation.

3.5 Model Validation and Accuracy Assessment

Model validation was performed using borehole yield and lithological data from 55 wells obtained from the Gombe State Water Corporation and the Water, Sanitation and Hygiene (WASH) programme. Boreholes were classified as productive (≥ 2 L/s) or non-productive (< 2 L/s) based on established yield thresholds for sustainable groundwater abstraction. Groundwater Potential Index (GPI) values were extracted at borehole locations and evaluated using Receiver Operating Characteristic (ROC) curve analysis and Area Under the Curve (AUC) statistics, implemented in Python (scikit-learn library).

By assessing the distribution of productive boreholes across the delineated groundwater potential classes, a success rate analysis was conducted. Result show a higher concentration of productive boreholes in the high and very high potential zones, confirming a strong spatial agreement between predicted groundwater potential and observed borehole yields.

4. Results and Discussion

4.1 Derived Thematic Layers

Eight thematic layers were derived from remote sensing and GIS analyses. Each parameter contributes uniquely to the hydrogeological conditions that influence groundwater occurrence and movement. These layers are: geology, slope, lineament density, drainage density, soil, land use/land cover (LULC), elevation, and rainfall.

4.1.1 Lineament Density

Lineament density in the area ranged from 0-100 km/km^2 (Figure 4.0A). Higher densities were noticed in the northeastern and southwestern zones. The dominant NE–SW orientation observed in the area corresponds with the regional tectonic trend of the Upper Benue Trough. These structurally deformed zones exhibit enhanced secondary porosity, facilitating infiltration and recharge around areas such as Wuro Ali Magini, Kulalum, and Wuro Biriji (Sener et al., 2005; Solomon and Quiel, 2006). Therefore, areas with high lineament density correspond to zones of high groundwater potential. The generated rose diagram (Figure 4.0 I) shows well-defined structural orientations at depth that closely match the predominant regional trends (E–W, NE–SW, NW–SE, and N–S) associated with the popular Zambuk Ridge. This structural framework exerts significant control over groundwater flow patterns and the configuration of the aquifer systems in the area.

4.1.2 Slope

Slope gradients derived from the DEM ranged between 0°-10° in the plains to over 20° in the uplands (Figure 4.0 B). Slopes that are gentle encourage infiltration and groundwater storage as it gives water ample time to go down, whereas steep slopes enhance runoff therefore limiting recharge (Jha et al., 2007). On the map, the central parts of Gombe, characterised by gentle topography, promote infiltration, while the western highlands and northeastern escarpments with steep slopes around Wuro Biriji and north of Kulalum, respectively, correspond to poor recharge areas.

4.1.3 Drainage Density

The inverse relationship between drainage density and infiltration capacity reinforces its significance as a key control on recharge (Figure 4.0 F). The drainage density observed ranged from 0.3-3.2 km/km^2. Low density areas (<1.2 km/km^2) in the central and northern sectors (Wuro Biriji) indicate permeable surface, whereas high-density areas in the southeastern zones (Arowa and Pantame) reflect low permeability and high runoff potential (Nag, 1998; Magesh et al., 2012).

4.1.4 Elevation

The elevation varies from 350 to 650 m, with low-lying central plains (e.g.,

Gombe and Arawa) coinciding with depositional environments favourable for recharge. The elevated regions in the west and around the inlier up north show reduced infiltration due to steep gradients and compact lithology (Murthy, 2000). The elevation pattern supports topographically driven groundwater convergence toward the central plains (Figure 4.0 G).

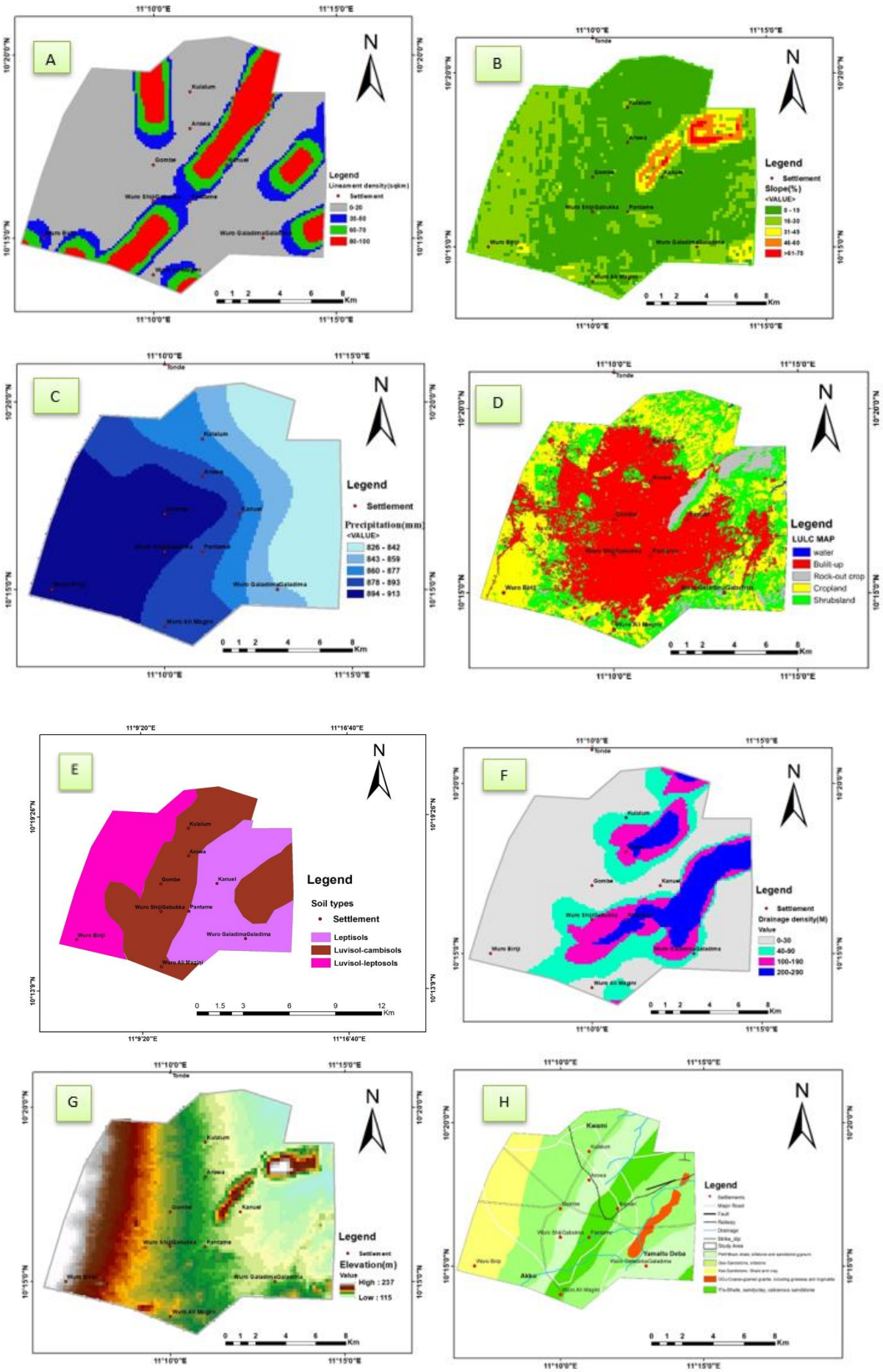

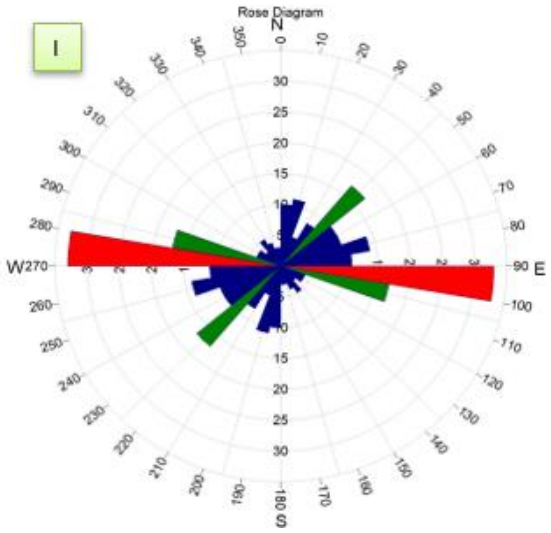

Figure 4: Thematic maps of groundwater conditioning factors: (A) Lineament density map, (B) Slope map, (C) Rainfall map, (D) Landuse land cover map, (E) Soil map, (F) Drainage density map, (G) Elevation map, (H) Geology map, and (I) Rose diagram

4.1.5 Geology

Five lithological units were mapped (Figure 4.0 H).

- Shale, siltstone, gypsum, and sandstone;
- Sandstone and siltstone;
- Shale, clay, and sandstone;
- Granite, gneiss, and migmatite;
- Shale, sandy clay, and sandstone.

Sedimentary formations, especially the Gombe and Kerri-Kerri Formations, around parts of Gombe and Wuro Biriji exhibit intergranular porosity and permeability, yielding higher groundwater potential (Offodile, 2002; Bala et al., 2011). In contrast, basement terrains around Gombe and Kwami display low primary porosity, with groundwater restricted to fractured zones (Mogaji et al., 2014).

4.1.6 Land Use/Land Cover (LULC)

The classified LULC map revealed five classes: cropland, scrubland, built-up area, rock outcrop, and water body (Figure 4.0D). Vegetated and agricultural land generally increase infiltration into soil, reduces runoff, and helps maintain soil structure and porosity. This by extension facilitates groundwater recharge. In contrast, urbanised areas like Gombe, Wuro Siji Gabukka, Pantami, and exposed rocky surfaces north of Kanuel,

restrict recharge by reducing infiltration capacity (Kumar et al., 2020). The continued expansion of Gombe city has consequently diminished recharge potential within built-up zones, while surrounding rural areas still retain comparatively higher infiltration rates.

4.1.7 Rainfall

Rainfall is the primary source of groundwater recharge, especially in areas with permeable soil and suitable geology. Interpolated mean annual rainfall for years 2020–2023 generated ranged from 850 - 1,000 mm, increasing westward (Figure 4.0 C). Areas with higher rainfall (Wuro Biriji and Gombe) coincide with permeable formations and moderate lineament density, leading to greater recharge potential (Gidey et al., 2017). Despite erratic seasonal rainfall, its alignment with high-infiltration terrain enhances recharge efficiency.

4.1.8 Soil

Three distinctive soil units were identified in the study area.

- **Leptosols unit:** characterised by shallow soil profile, low storage capacity and fracture-controlled infiltration. Hence, localised and low groundwater recharge (Kanuel and Galadima)
- **Luvisol-cambisols unit** exhibits moderate to high water retention with balanced infiltration and storage. Areas around Wuro baji and north of it have this soil type.
- **Luvisol-leptosols unit:** poorly drained, also possesses low groundwater potential like Leptosols

So, towns like Gombe, kulalum and Aruwo have low potentials while Pantami, Wuro Biriji and Kanuel would have higher potentials.

4.2 Weighting Results, (AHP)

The AHP pairwise comparison matrix (Table 2) yielded consistent and robust weight values (CR = 0.011). The lineament density (0.276) and rainfall (0.215) emerged as the most influential factors, followed by geology (0.168) and drainage density (0.131). These results emphasise the dominance of structural and climatic controls on groundwater occurrence within the study area. Lineaments control recharge pathways, while rainfall provides the primary input for infiltration. Slope, soil type, and elevation show relatively lower weights (secondary influence). The derived weights align very closely with (Rahmati et al., 2016; Igwe et al., 2020).

Table 2: Pairwise comparison matrix

	A	B	C	D	E	F	G	H
A	1.000000	4.000000	0.333333	5.000000	0.500000	6.000000	5.000000	6.000000
B	0.250000	1.000000	0.200000	3.000000	0.200000	4.000000	2.000000	4.000000
C	3.000000	5.000000	1.000000	6.000000	2.000000	6.000000	6.000000	6.000000
D	0.200000	0.333333	0.166667	1.000000	0.166667	2.000000	0.500000	3.000000
E	2.000000	5.000000	0.500000	6.000000	1.000000	6.000000	5.000000	6.000000

Table 2 (cont): Pairwise comparison matrix								
F	0.166667	0.250000	0.166667	0.500000	0.166667	1.000000	0.333333	2.000000
G	0.200000	0.500000	0.166667	2.000000	0.200000	3.000000	1.000000	4.000000
H	0.166667	0.250000	0.166667	0.333333	0.166667	0.500000	0.250000	1.000000

Where: A = Geology, B = Drainage Density, C = Lineament Density, D = Land use and Land cover, E = Rainfall, F = Slope, G = Soil type, and H = Elevation.

Table 3: Normalised AHP weights for groundwater conditioning factors	
Criteria	**AHP Weight**
Geology	0.168143
Drainage Density	0.131465
Lineament Density	0.276347
Land Use/Land Cover	0.054335
Rainfall	0.215186
Slope	0.048749
Soil Type	0.060851
Elevation	0.044924
Total	**1**

4.3 Groundwater Potential Zonation

The weighted overlay analysis generated a Groundwater Potential Index (GPI) map that classified the area from into four classes (very low to high) potential zones, with about 45% of the region falling within moderate to high potential and 55% within low to very low potential. High potential areas are mainly in the western and central parts, including Wuro Biriji, Kulalum, and Gombe town, where sandstone formations, gentle slopes, and dense fracture networks enhance recharge. In contrast, low potential zones in northeastern Gombe and Kwami correspond to basement outcrops and steep terrains that limit infiltration. Overall, the results highlight the strong influence of geology, structure, and topography on groundwater distribution across the area.

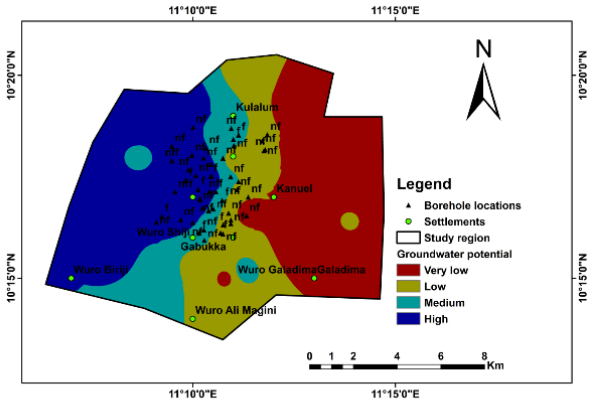

Figure 5: Groundwater potential map showing borehole points

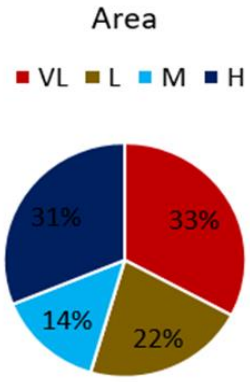

Figure 6: groundwater distribution pie chart

Table 4: Groundwater distribution percentage.

Class	Area (km^2)	Percentage (%)
Very Low	46.01	33
Low	30.48	22
Moderate	20.01	14
High	43.66	31

The distribution pattern shows that areas of medium to high potential correspond to sedimentary formations, while low-potential zones coincide with crystalline basement terrains. This pattern is consistent with field observations of borehole yields and with other studies in the Upper Benue Trough (Bala et al., 2018; Yelwa et al., 2018).

4.4 Model Validation and Performance Assessment

The model was validated using yield data from 55 boreholes (Table 5). Result obtained demonstrates a strong predictive performance of the groundwater potential model. About 81% of the productive boreholes were noticed to be located within zones classified as high - moderate groundwater potential. Thus, indicating good spatial agreement between observed borehole yields and the AHP-derived groundwater potential map. Furthermore, the ROC analysis produced an AUC value of 0.52, which reflects a very good discrimination between productive and non-productive zones therefore, confirming the robustness of the model (Fawcett, 2006). This result corresponds to similar RS–GIS–AHP groundwater potential assessment studies in other semi-arid and hard rock regions (Rahmati et al., 2016; Igwe et al., 2020).

Furthermore, success-rate analysis revealed a proportional increase in borehole productivity with higher GPI classes, reinforcing the model's internal consistency. The model thus provides a scientifically credible and operationally useful tool for groundwater resource planning in Gombe and other similar environments.

Table 5: Borehole Data

LAT	LON	BH No	Name of community	BH types	year	BH Depth	Yield	Status
10.2777166	11.1735239	B1	Bolari west	MBH	2018	48	0	not functioning
10.2776525	11.1733144	B2	Bolari west	MBH	2010	30	0	not functioning
10.2783947	11.1754394	B3	Bolari east	MBH	2016	45		not functioning
10.2901933	11.1640967	B4	Jakada fari modibo tukur	SBH	2021 FGN	78	0	not functioning
10.2902138	11.1640817	B5	Jakada fari modibo tukur	SBH	2021 FGN	78	0	FUNCTIONING
10.2901013	11.1640887	B6	Jakada fari modibo tukur	SBH	2021	78	0	FUNCTIONING
10.2901817	11.1641145	B7	Jakada fari modibo tukur	SBH	2021	78	0	FUNCTIONING
10.2724492	11.1825871	B8	Bolari east, marafan Bolari	SBH	2017	78	0	FUNCTIONING
10.2739212	11.1826084	B9	Malam saleh, Bolari east	MBH	2017 FGN	54	0	not functioning
10.2787244	11.1709062	B10	Near alhaji Balulu house,	SBH	2018 fgn	54	0	not functioning
10.2822437	11.1699227	B11	Korafi musa mai taya	MBH	2024, state	78	0	not functioning
10.2901765	11.1641054	B12	Jakada fari modibo tukur	SBH	2021 FGN	78	0	FUNCTIONING
10.2982691	11.1583533	B13	Kasuwan shanu community,Shamaki	MBH	2009 state	66	1	FUNCTIONING
10.2756894	11.1889899	B14	Madaki residence, bolari east, Jakada	SBH	2018 state	54	0	not functioning
10.2684797	11.1695591	B15	Alhaji saidu mai kusa st. Pantami	MBH	1980, state	100	0	FUNCTIONING
10.2871950	11.1617617	B16	nil	nil	nil	nil	nil	nil
10.2753942	11.1542164	B17	Buhari quarters, Pantami Abuja	MBH	1979	96	0	FUNCTIONING
10.2728483	11.1669085	B18	Malam adamu kwanan Plato Pantami	MBH	2016,, FGN	54	0	Functioning
10.2854643	11.1597054	B19	layin nayaya Jakada Fari	SBH	2021, STATE	90	0	NOT FUNCTIONING
10.2729700	11.1692467	B20	nil	nil	nil	nil	nil	nil
10.2729997	11.1693473	B21	emirs palace, Pantami	MBH	2012, others	27	0	not functioning
10.2745050	11.1679495	B22	nil	nil	nil	nil	nil	nil
10.2656169	11.1717089	B23	Dokoro old house Pantami	MBH	2017 FGN	90	0	FUNCTIONING
10.2699139	11.1714971	B24	Bappa jalo barambu st. Pantami	MBH	2018, state	78	0	functioning
10.2700040	11.1709271	B25	nil	nil	nil	nil	nil	nil
10.2718873	11.1794009	B26	Behind muazu Mai Sharia residence par	SBH	2021 FGN	68	0	FUNCTIONING
10.2686459	11.1783467	B27	Abubakar hina str. Pantami	sbh	2013 state	99	0	functioning
10.2682011	11.1793601	B28	Marafa str. Pantami	SBH	2022 FGN	72	0	FUNCTIONING
10.3027241	11.1967224	B29	KagawalPHC1, SHAMAKI	MBH	2019, OTHERS	48	0	FUNCTIONING
10.3023717	11.1962083	B30	KagawalPHC2, SHAMAKI	SBH	2019 FGN	58	0	not functioning
10.3011550	11.1825600	B31	nil	nil	nil	nil	nil	nil
10.3088523	11.1858156	B32	Lafiyawo mala inna, shamaki	MBH	1979 FGN	108	8	not functioning
10.3167950	11.1645450	B33	Nil	nil	nil	nil	nil	nil
10.2993737	11.1714228	B34	Malam inuwa layi gobnan yobe, shamak	MBH	2007 OTHERS	48	0.5	FUNCTIONING
10.2981428	11.1583768	B35	Kasuwan shanu community,Shamaki	MBH	2009, state	66	1	FUNCTIONING
10.3070087	11.1836200	B36	malam inna Almajiri sch. Tsangaya	mbh	2012 fgn	60	0	FUNCTIONING
10.3045017	11.1838583	B37	Sabon fagin malam inna shamaki	SBH	2009 FGN	86	0	not functioning
10.3087867	11.1857733	B38	lafiawo malan inna community Shamak	mbh	1979 fgn	96	0.5	FUNCTIONING
10.3114967	11.1827733	B39	Mai Angwa Kwaranga	mbh	2015 state	36	0.5	FUNCTIONING
10.3063637	11.1955126	B40	sarkin gabas kagarawal, shamaki	SBH	2021 FGN	128	10	FUNCTIONING
10.3075250	11.1896467	B41	nil	nil	nil	nil	nil	nil
10.3119669	11.1670361	B42	JAURO ABARE KORON ZAKI COMM, SHA	mbh	2007 state	96	0	not functioning
10.3089574	11.1975853	B43	Kagarawal rumbe comm,shamaki ward	SBH	1978 FGN	84	0	not functioning
10.2929450	11.1714233	B44	nil	nil	nil	nil	nil	nil
10.2936300	11.1777450	B45	nil	nil	nil	nil	nil	nil
10.2827383	11.1698867	B46	KOFAR ALHAJI MUSA DAN GWMGWAM,	SBH	2021 FGN	120	0	not functioning
10.2967933	11.1745140	B47	Gandu junior section, shamaki	mbh	2018 state	108	0	FUNCTIONING
10.2959009	11.1779056	B48	vocational sec sch shamaki	mbh	2021 state	66	nil	FUNCTIONING
10.2992851	11.1793532	B49	Gov comp day sec sch. Shamaki	sbh	2020 state	68	0	FUNCTIONING
10.2928170	11.1889916	B50	nil	nil	nil	nil	nil	nil
10.2833024	11.1897298	B51	State Medical Store Gombe dawaki war	mbh	2007 state	54	0	FUNCTIONING
10.2896191	11.1857602	B52	Along rail way Quaters dawaki ward	MBH	1992 state	108	0	not functioning
10.2863114	11.1851782	B53	Railway police barrack Herwagana ward	MBH	1978 fgn	52	0	FUNCTIONING
10.2942986	11.1745122	B54	Layin Amadu Mai kifi bajoga ward bajog	SBH	2013 fgn	78	0	FUNCTIONING
10.2855483	11.1764667	B56	MAI ANGUWA BACHI COMMUNITY herw	MBH	2020 state	78	16	FUNCTIONING
10.3042211	11.1583040	B57	SPECIAL EDUCATION CENTER GOMBE BC	SBH	2021 others	72	0	not functioning
10.2864712	11.1691419	B58	HASSAN CENTRAL PRIMARY SCH. Shama	SBH	2015 fgn	86	16	FUNCTIONING
10.2918894	11.1743193	B59	Al imam Malik community Islamic acade	MBH	2017 FGN	90	0	FUNCTIONING
10.2917915	11.1747614	B60	Dawaki Layin Alaramma mallam bala	MBH	2021 others	75	0	FUNCTIONING
10.2920922	11.1681920	B61	Modibbo bubayero secretariat and Islar	MBH	2023 state	78	0	not functioning
10.2732920	11.1798824	B62	nil	nil	nil	nil	nil	nil
10.2767102	11.1816600	B63	Abuja Quaters haruna mamuda residen	MBH	1978 fgn	66	0	not functioning
10.2916624	11.1825097	B64	Opposite Garkuwa school of health and	MBH	1978 fgn	78	0	not functioning
10.2944592	11.1651491	B65	Layin uban doma bajoga ward bajoga	MBH	2018 fgn	78	0	FUNCTIONING
10.2856957	11.1738768	B66	KOFAR DAGACI BABAYO COMMUNITY B	MBH	2021 othres	108	nil	FUNCTIONING
10.2855733	11.1738150	B55	KOFAR DAGACI COMMUNITY 2 HERWAG	MBH	2001 state	96	0	not functioning
10.2915250	11.1823963	B67	nil	nil	nil	nil	nil	nil
10.3005084	11.1666438	B68	LAYIN INJI UKU SHAMAKI WARD	MBH	2018 others	60	0	functioning
10.2905900	11.1563600	B69	nil	nil	nil	nil	nil	nil
10.3034302	11.1723836	B70	GSU NITDA ICT PACK BOREHOLE 2	MBH	2013 fgn	50	4	not functioning
10.3072238	11.1742194	B71	NEAR PHARMACY DEPARTMENT GSU sha	MBH	2013 fgn	65	nil	FUNCTIONING

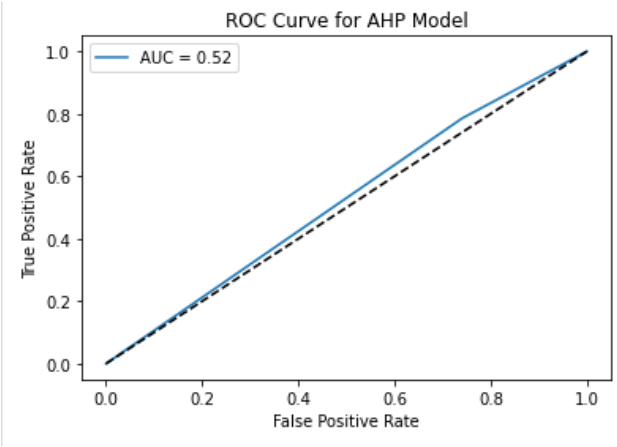

Figure 5: ROC curve for model validation (AUC = 0.52).

4.5 Discussion of Hydrogeological Implications

The study confirms that groundwater potential in Gombe and its environs is primarily controlled by lithology, structural deformation, and topography. Sandstone formations associated with fracture networks favour recharge and storage, while crystalline basement areas show low yield potential except where lineament density is high. Data resolution and variability in rainfall may bring uncertainties.

Incorporating geophysical validation methods, such as VES, could enhance accuracy. Overall, the approach demonstrates strong predictive power and adaptability for groundwater studies in comparable hydrogeological settings.

5. Conclusion

This study employed an integrated framework of Remote Sensing (RS), Geographic Information System (GIS), and Artificial Intelligence (AI) approach to evaluate groundwater potentials in Gombe and its environs using eight key parameters. These include: geology, lineament density, slope, drainage density, soil, land use/land cover, elevation, and rainfall. They were combined to generate a Groundwater Potential Index (GPI) map using the Analytical Hierarchy Process (AHP), an AI-based decision-support algorithm that reduced subjectivity and improved consistency in factor prioritization. The resulting groundwater potential index (GPI) map classified the area into very low to high potential zones.

Results revealed that lithology, structural lineament, slope, and drainage density are the dominant controls on groundwater occurrence. High-medium potential zones occur mainly in the eastern part of the map (Kanuel and Galadima), while low-potential zones correspond to the thick kerri kerri part of the study area. Borehole yield is most likely determined by lithology and depth of the boreholes. Model validation using borehole yield data and ROC–AUC machine learning metrics confirmed strong predictive performance, with 81% of productive boreholes located within moderate-to-high potential zones. This demonstrates that AI-driven weighting and validation significantly enhance the reliability of RS–GIS groundwater mapping.

This study shows that RS–GIS–with AI technique integration offers a reliable, transferable and cost-effective approach to groundwater exploration and management in data-scarce and geologically complex terrains. It recommends drilling around the high-potential areas for borehole. Overall, the research addresses water resource planning in part of Gombe State and provides a model that could be transferred to similar semi-arid regions in Africa.

It is important to note that while artificial intelligence techniques such as AHP weighting and ROC–AUC validation were incorporated, they account for less than 30% of the methodology, with over 70% of the work grounded in conventional Remote Sensing (RS), GIS, and hydrogeological analysis.

References

Abdullahi, A. M., and Saidu, A. M., 2020. Assessment of groundwater potential zones in semi-arid environments using remote sensing and GIS techniques. Journal of African Earth Sciences, 167, 103857. https://doi.org/10.1016/j.jafrearsci.2020.103857

Bala, A. E., Ike, E. C., and Balogun, I., 2011. Geoelectric investigation of groundwater potential of Gombe and environs, northeastern Nigeria. Journal of Applied Sciences and Environmental Management, 15(1), Pp. 9–14.

Bala, A. E., Olayinka, A. I., and Shemang, E. M., 2018. Geoelectrical characterization of aquifers in the Upper Benue Trough, northeastern Nigeria. Hydrogeology Journal, 26(4), Pp. 973–988. https://doi.org/10.1007/s10040-017-1712-4

Burrough, P. A., and McDonnell, R. A., 1998. Principles of geographical information systems (2nd ed.). Oxford University Press.

Drusch, M., Del Bello, U., Carlier, S., Colin, O., Fernandez, V., Gascon, F., Hoersch, B., Isola, C., Laberinti, P., Martimort, P., Meygret, A., Spoto, F., Sy, O., Marchese, F., and Bargellini, P., 2012. Sentinel-2: ESA's optical high-resolution mission for GMES operational services. Remote Sensing of Environment, 120, Pp. 25–36. https://doi.org/10.1016/j.rse.2011.11.026

Fawcett, T., 2006. An introduction to ROC analysis. Pattern Recognition Letters, 27(8), Pp. 861–874. https://doi.org/10.1016/j.patrec.2005.10.010

Gidey, E., Teka, A., Gebreslasie, M., and Hagos, M., 2017. Delineation of groundwater potential zones using GIS and remote sensing techniques: A case study from Northern Ethiopia. Journal of African Earth Sciences, 134, Pp. 141–154.

Igwe, O., Nwankwoala, H. O., and Onwuemesi, A. G., 2020. Application of GIS and AHP for groundwater potential mapping in crystalline basement terrains of southeastern Nigeria. Environmental Earth Sciences, 79(8), Pp. 198. https://doi.org/10.1007/s12665-020-08939-9

Jha, M. K., Chowdhury, A., Chowdary, V. M., and Peiffer, S., 2007. Groundwater management and development by integrated remote sensing and GIS: Prospects and constraints. Water Resources Management, 21(3), Pp. 427–467. https://doi.org/10.1007/s11269-006-9024-4

Kumar, P., Das, J., and Mukherjee, S., 2020. Assessment of groundwater potential zones using remote sensing, GIS and multi-criteria decision-making techniques in a semi-arid region of India. Environmental Earth Sciences, 79(16), Pp. 412.

Kumar, T. S., and Krishna, A. K., 2018. Integration of AHP and GIS for delineating groundwater potential zones in hard rock terrains. Hydrological Sciences Journal, 63(9), Pp. 1353–1366. https://doi.org/10.1080/02626667.2018.1503499

Magesh, N. S., Chandrasekar, N., and Soundranayagam, J. P., 2012. Delineation of groundwater potential zones in Theni district, Tamil Nadu, using remote sensing, GIS and MIF techniques. Geoscience Frontiers, 3(2), Pp. 189–196.

Mogaji, K. A., Omosuyi, G. O., and Abijoye, T., 2014. Groundwater potential mapping using GIS and geophysical data: A case study of basement complex terrain of southwestern Nigeria. Environmental Earth Sciences, 71(8), Pp. 3523–3537.

Mulder, V. L., de Bruin, S., and Schaepman, M. E., 2011. Monitoring soil properties using remote sensing. Remote Sensing of Environment, 115(11), Pp. 3078–3089. https://doi.org/10.1016/j.rse.2011.06.017

Murthy, K. S. R., 2000. Groundwater potential in a semi-arid region of

Andhra Pradesh: A geographical information system approach. International Journal of Remote Sensing, 21(9), Pp. 1867–1884.

Nag, S. K., 1998. Morphometric analysis using remote sensing techniques in the Chaka sub-basin, Purulia district, West Bengal. Journal of the Indian Society of Remote Sensing, 26(1–2), Pp. 69–76.

Nag, S. K., and Lahiri, A., 2012. Lineament mapping and its correlation with fractures and mineral occurrences, Satpura Plateau, India: Using remote sensing and GIS. International Journal of Remote Sensing and GIS, 1(2), Pp. 77–88.

Offodile, M. E., 2002. Groundwater study and development in Nigeria (2nd ed.). Mecon Geology and Engineering Services Ltd.

Rahmati, O., Nazari Samani, A., Mahdavi, M., Pourghasemi, H. R., and Zeinivand, H., 2015. Groundwater potential mapping at Kurdistan region of Iran using analytic hierarchy process and GIS. Arabian Journal of Geosciences, 8(9), Pp. 7059–7071.

Rahmati, O., Pourghasemi, H. R., and Melesse, A. M., 2016. Application of GIS-based multi-criteria decision analysis for groundwater potential mapping. Environmental Earth Sciences, 75(9), Pp. 752. https://doi.org/10.1007/s12665-016-5556-8

Saaty, T. L., 1980. The analytic hierarchy process: Planning, priority setting, resource allocation. McGraw-Hill.

Sener, E., Davraz, A., and Ozcelik, M., 2005. An integration of GIS and remote sensing in groundwater investigations: A case study in Burdur, Turkey. Hydrogeology Journal, 13(5–6), Pp. 826–834. https://doi.org/10.1007/s10040-004-0378-5

Shalaby, A., and Tateishi, R., 2007. Remote sensing and GIS for mapping and monitoring land cover and land-use changes in northwestern Egypt. Applied Geography, 27(1), Pp. 28–41. https://doi.org/10.1016/j.apgeog.2006.09.004

Solomon, S., and Quiel, F., 2006. Groundwater study using remote sensing and GIS in the central highlands of Eritrea. Hydrogeology Journal, 14(6), Pp. 1029–1041.

Todd, D. K., and Mays, L. W., 2004. Groundwater hydrology (3rd ed.). John Wiley and Sons.

Yelwa, N. A., Ibrahim, Y. K., and Gwarzo, U. S., 2018. Groundwater potential assessment using geoelectric and GIS techniques in parts of the Upper Benue Trough, northeastern Nigeria. Journal of African Earth Sciences, 145, Pp. 240–252.